

Lecture 6

I. Non-ideal operational amplifiers

Equations (5.47) and (5.48) for the amplifier gains with the voltage feedback are valid only if the voltage open loop gain is infinite. It is sometimes important to consider a physical amplifier which does not satisfy this restriction. In Fig. 1, the inverting amplifier is described by its small-signal model, with the open loop gain $\hat{A}(\omega) \neq 0$, $R_{in} \neq 0$, and $R_{out} \neq 0$. Also, an input shunting capacitor C is included to this model.

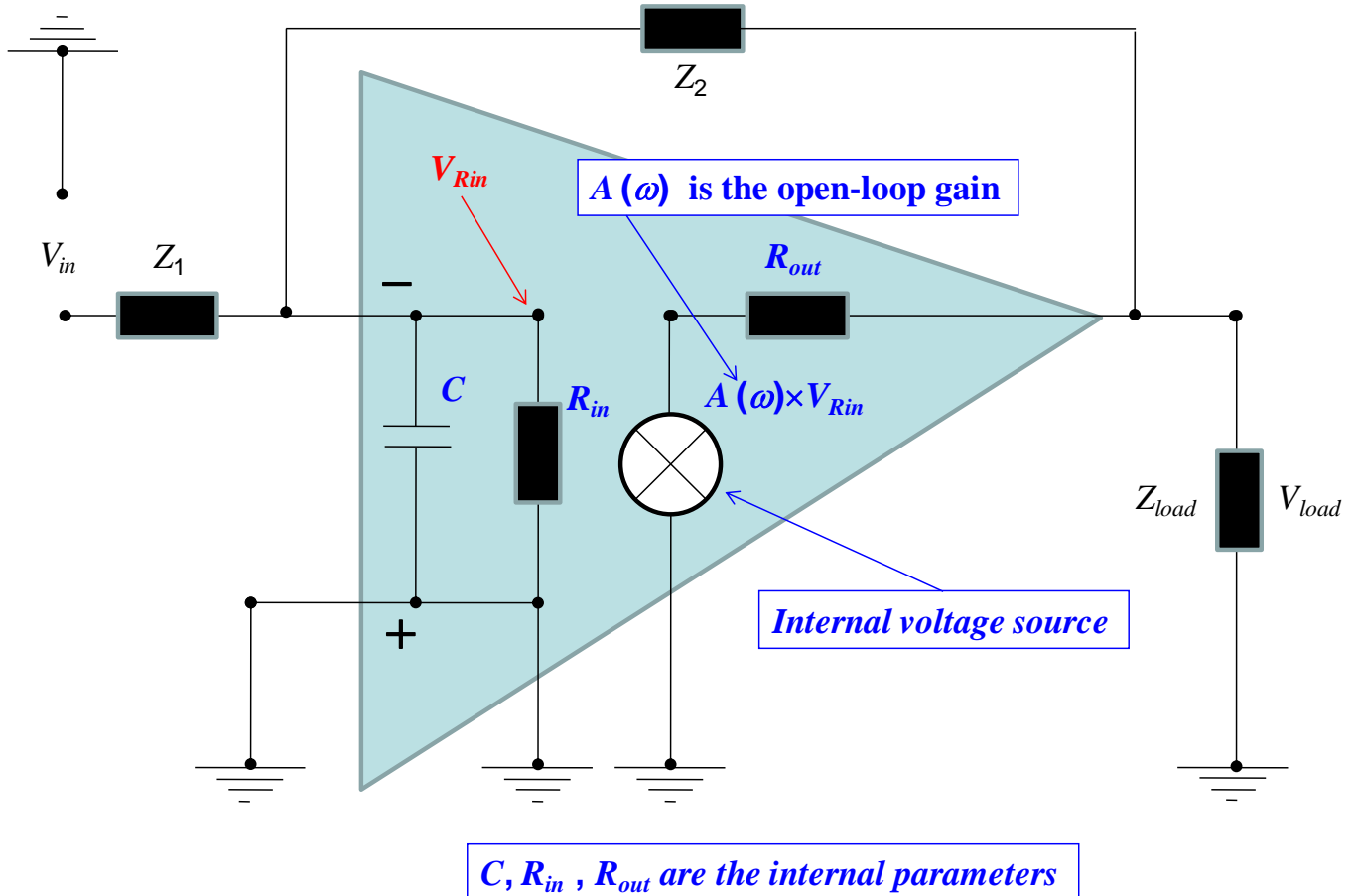


Fig. 1 A small signal model (one of many other possible) of the non-inverting operational amplifier.

In Fig. 1, $V_{R_{in}}$ is the voltage across R_{in} , $\hat{A}(\omega) \times V_{R_{in}}$ is the equivalent voltage source, Z_{load} is any load impedance, Z_1 and Z_2 are any feedback impedances. Note that any impedance may depend on the frequency. We will calculate the feedback gain $\hat{A}_f^-(\omega)$ for this model. The circuit diagram of this amplifier is shown in the Fig. 2.

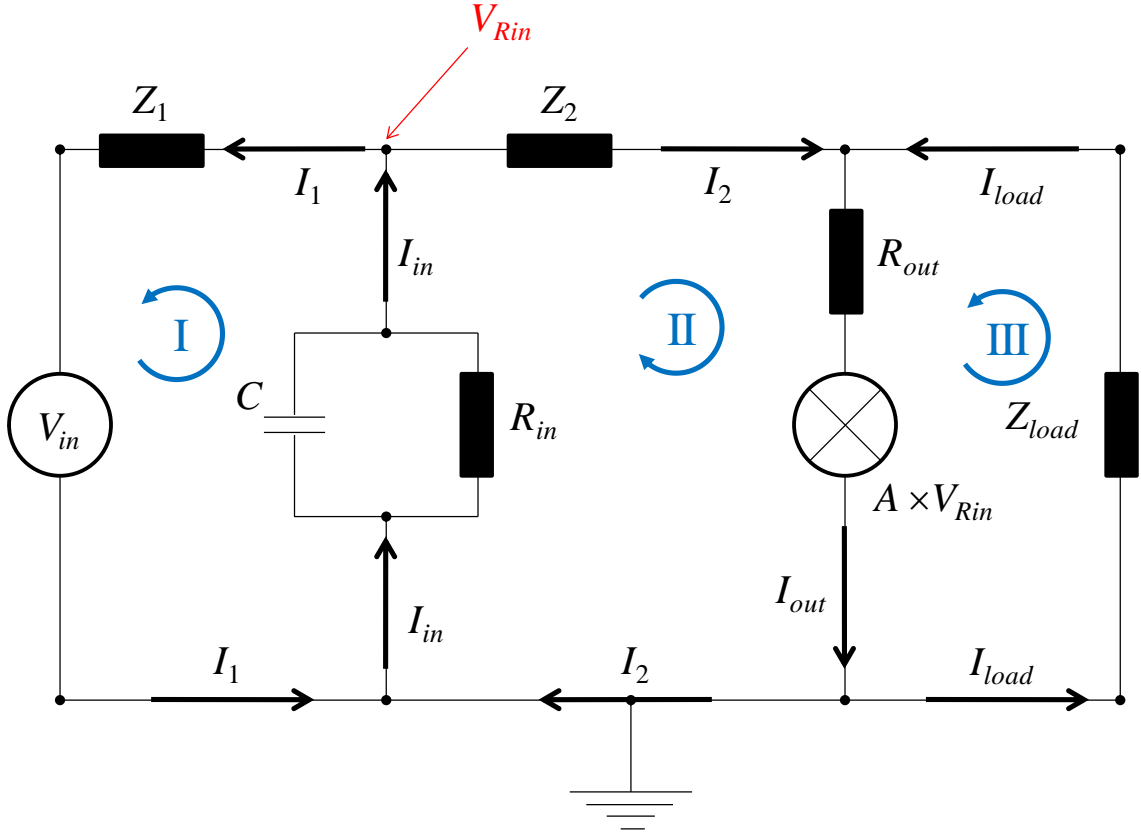


Fig. 2 The circuit diagram of the amplifier shown in the Fig. 1.

Using Kirchhoff's voltage and current laws for the circuit loops I, II, and III, we obtain the following system in the frequency domain (the loop directions are conventional):

$$\left\{ \begin{array}{l} V_{in} = V_1 + V_{R_{in}} \\ \hat{A} V_{R_{in}} = V_{out} + V_2 + V_{R_{in}} \\ \hat{A} V_{R_{in}} = V_{load} + V_{out} \\ \frac{V_{R_{in}}}{Z_{in}} = \frac{V_1}{Z_1} + \frac{V_2}{Z_2} \\ \frac{V_{out}}{R_{out}} = \frac{V_2}{Z_2} + \frac{V_{load}}{Z_{load}} \end{array} \right. \quad (1)$$

Where, V_1 is the voltage across Z_1 , V_2 is the voltage across Z_2 , V_{out} is the voltage across R_{out} , V_{load} is the voltage across Z_{load} , $Z_{in} = \frac{R_{in}}{1 + iR_{in}C\omega}$ is the input impedance ($\exp(+i\omega t)$ time dependence is used),

and $\frac{V_{R_{in}}}{Z_{in}} = I_{in}$, $\frac{V_1}{Z_1} = I_1$, $\frac{V_2}{Z_2} = I_2$, $\frac{V_{out}}{Z_{out}} = I_{out}$, and $\frac{V_{load}}{Z_{load}} = I_{load}$ are the branch currents. The voltages

$V_{R_{in}} = V_{in} - V_1$ and $V_{out} = \frac{R_{out}}{Z_2} V_2 + \frac{R_{out}}{Z_{load}} V_{load}$ can be excluded from Eq. (1):

$$\begin{cases} V_{in}(\hat{A}-1) = (\hat{A}-1)V_1 + \left(\frac{R_{out}+Z_2}{Z_2}\right)V_2 + \left(\frac{R_{out}}{Z_{load}}\right)V_{load} \\ V_{in}\hat{A} = \hat{A}V_1 + \left(\frac{R_{out}}{Z_2}\right)V_2 + \left(\frac{R_{out}+Z_{load}}{Z_{load}}\right)V_{load} \\ V_{in} = \left(\frac{Z_1+Z_{in}}{Z_1}\right)V_1 + \left(\frac{Z_{in}}{Z_2}\right)V_2 \end{cases} \quad (2)$$

The system of equations (2) can be rewritten in the matrix form:

$$\hat{\mathbf{B}} \begin{pmatrix} V_1 \\ V_2 \\ V_{load} \end{pmatrix} = \begin{pmatrix} V_{in}(\hat{A}-1) \\ V_{in}\hat{A} \\ V_{in} \end{pmatrix} \quad (3)$$

where

$$\hat{\mathbf{B}} = \begin{pmatrix} (\hat{A}-1) & \left(\frac{R_{out}+Z_2}{Z_2}\right) & \left(\frac{R_{out}}{Z_{load}}\right) \\ \hat{A} & \left(\frac{R_{out}}{Z_2}\right) & \left(\frac{R_{out}+Z_{load}}{Z_{load}}\right) \\ \left(\frac{Z_1+Z_{in}}{Z_1}\right) & \left(\frac{Z_{in}}{Z_2}\right) & 0 \end{pmatrix} \quad (4)$$

$$\det \hat{\mathbf{B}} = \frac{(R_{out}+Z_2)(Z_{load}+R_{out})(Z_1+Z_{in}) - R_{out}^2(Z_1+Z_{in}) + Z_{in}Z_1(Z_{load}+R_{out}) - A_V Z_1 Z_{in} Z_{load}}{Z_1 Z_2 Z_{load}} \quad (5)$$

The inverse matrix $\hat{\mathbf{B}}^{-1}$ can be calculated using the complementary minors $\{M_{ij}\}$:

$$\hat{\mathbf{B}}^{-1} = \{b_{ij}^{-1}\} = \frac{1}{\det \hat{\mathbf{B}}} \{(-1)^{i+j} M_{ji}\} \quad (6)$$

Here, $\{M_{ji}\}$ is the transposed matrix $\{M_{ij}\}$:

$$\begin{aligned}
(-1)^{i+i} M_{ji} = & \begin{pmatrix} -\frac{(Z_{load} + R_{out})Z_{in}}{Z_{load}Z_2} & \frac{R_{out}Z_{in}}{Z_{load}Z_2} & \frac{(R_{out} + Z_2)(Z_{load} + R_{out}) - R_{out}^2}{Z_2Z_{load}} \\ \frac{(Z_{load} + R_{out})(Z_1 + Z_{in})}{Z_1Z_{load}} & -\frac{R_{out}(Z_1 + Z_{in})}{Z_1Z_{load}} & \frac{\hat{A}R_{out} - (\hat{A} - 1)(Z_{load} + R_{out})}{Z_{load}} \\ \frac{\hat{A}Z_{in}Z_1 - R_{out}(Z_1 + Z_{in})}{Z_1Z_2} & \frac{(R_{out} + Z_2)(Z_1 + Z_{in}) - (\hat{A} - 1)Z_{in}Z_1}{Z_1Z_2} & \frac{(\hat{A} - 1)R_{out} - \hat{A}(R_{out} + Z_2)}{Z_2} \end{pmatrix} \\
& (7)
\end{aligned}$$

The unknown vector $\begin{pmatrix} V_1 \\ V_2 \\ V_{load} \end{pmatrix} = \hat{\mathbf{B}}^{-1} \begin{pmatrix} V_{in}(\hat{A} - 1) \\ V_{in}\hat{A} \\ V_{in} \end{pmatrix}$ can be calculated using (6) and (7). We need V_{load} :

$$V_{load} = V_{in} \frac{Z_{in}(R_{out} + \hat{A}Z_2)}{Z_1Z_2 \det \hat{\mathbf{B}}} \quad (8)$$

Or

$$\hat{A}_f^-(\omega) = \frac{V_{load}}{V_{in}} = \frac{Z_{load}Z_{in}(R_{out} + \hat{A}Z_2)}{(Z_2R_{out} + Z_2Z_{load} + R_{out}Z_{load})(Z_1 + Z_{in}) + Z_{in}Z_1(Z_{load} - \hat{A}Z_{load} + R_{out})} \quad (9)$$

For the ideal amplifier with $C = 0$ ($Z_{in} = R_{in}$), $R_{out} = 0$, $R_{in} \rightarrow \infty$, and $|\hat{A}| \rightarrow \infty$, we obtain from (9):

$$\hat{A}_f^-(\omega) = \frac{V_{load}}{V_{in}} = -\frac{Z_2(\omega)}{Z_1(\omega)}.$$

Using $Z_{in} = \frac{R_{in}}{1 + iR_{in}C\omega}$, Eq. (9) can be rewritten in the following form:

$$\hat{A}_f^-(\omega) = \frac{Z_{load}R_{in}(R_{out} + \hat{A}Z_2)}{(Z_2R_{out} + Z_2Z_{load} + R_{out}Z_{load})(Z_1 + R_{in} + iR_{in}CZ_1\omega) + Z_1R_{in}(Z_{load} - \hat{A}Z_{load} + R_{out})} \quad (10)$$

If all the parameters in Eq. (10) are real and $\hat{A} < 0$, $\hat{A}_f^-(\omega)$ will have only one pole $i\omega_1$ in the upper half plane:

$$i\omega_1 = \frac{i}{C} \left[\frac{Z_1 + R_{in}}{R_{in}Z_1} + \frac{Z_{load}(1 - \hat{A}) + R_{out}}{Z_2(R_{out} + Z_{load}) + R_{out}Z_{load}} \right] \quad (11)$$

Therefore, unavoidable internal capacitances in semiconductor chips will introduce the frequency dispersion and poles (one or more) in the amplifier gain even for a resistive feedback (Z_1 and Z_2 are real). In the model in Fig. 1, we have only one pole if all other parameters, including the feedback, are real. Such transfer function (with a resistive feedback) can be written as:

$$\hat{A}_f^-(\omega) = \frac{A_{0f}}{1 + i \frac{\omega}{\omega_1}} = \frac{-iA_{0f}\omega_1}{\omega - i\omega_1} \quad (12)$$

where $i\omega_1$ is the imaginary pole (11) and A_{0f} is some real constant. Using (4.53), we can calculate the time domain transfer function:

$$\begin{cases} A_f^{-1}(t > 0) = A_{0f}\omega_1 \exp(-\omega_1 t) \\ V_{out}(t) = \int_{-\infty}^t A_f^{-1}(t-s)V_{in}(s)ds = A_{0f}\omega_1 \int_{-\infty}^t \exp(-\omega_1(t-s))V_{in}(s)ds \end{cases} \quad (13)$$

This single pole transfer function introduces only the relaxation process without ringing oscillations. However, in the experiments with operational amplifiers we often observe ringing oscillations for a pulse excitation (if the gain is not too large). **Therefore, a practical amplifier should have two or more poles in the transfer function.** If in Eq. (11) $\hat{A} \rightarrow -\infty$, $R_{in} \rightarrow \infty$, and $R_{out} \rightarrow 0$, the pole $i\omega_1$ will disappear (move to the infinity):

$$i\omega_1 \rightarrow \frac{-i\hat{A}}{CZ_2} \quad (14)$$

This fact tells us that any poles in the ideal amplifier can be induced only by the impedance feedback circuit. In a practical amplifier, the open loop transfer function $\hat{A}(\omega)$ by itself will have one or more poles. For example, for a two pole $\hat{A}(\omega)$, we have:

$$\hat{A}(\omega) = \frac{A_0}{\left(1 + i \frac{\omega}{\omega_1}\right) \left(1 + i \frac{\omega}{\omega_2}\right)} \quad (15)$$

where $\omega_{1,2}$ are some complex poles in the upper half plane and A_0 is some real negative constant. Putting (15) to (9), we obtain:

$$\begin{cases} \hat{A}_f^-(\omega) = \frac{Z_{load}Z_{in}(R_{out}\hat{P}(\omega, \omega_1, \omega_2) + A_0Z_2)}{((Z_2R_{out} + Z_2Z_{load} + R_{out}Z_{load})(Z_1 + Z_{in}) + Z_{in}Z_1Z_{load} + R_{out}Z_{in}Z_1)\hat{P}(\omega, \omega_1, \omega_2) - A_0Z_{load}Z_{in}Z_1} \\ \hat{P}(\omega, \omega_1, \omega_2) = \left(1 + i \frac{\omega}{\omega_1}\right) \left(1 + i \frac{\omega}{\omega_2}\right) \end{cases} \quad (16)$$

Even for a resistive feedback, the transfer function in Eq. (16) will have two internal poles due to the polynomial $\hat{P}(\omega, \omega_1, \omega_2)$. **This transfer function may demonstrate ringing oscillations in the time domain for a sharp pulse excitation. The pole positions in the complex plane will be defined by all the parameters in the model equation (16), including the feedback and load impedances.**

Similar model approach can be developed for a non-inverting amplifier.

II. Common-mode rejection ratio (CMRR)

A practical operational amplifier is never perfectly “differential”, and hence the output signal will depend not only on the differential signal ΔV , but also on the input signal magnitudes V_1 and V_2 , each measured with respect to ground. In this case, instead of one open loop gain we will have two gains (frequency domain):

$$\hat{V}_{out}(\omega) = \hat{A}_1(\omega)\hat{V}_1(\omega) + \hat{A}_2(\omega)\hat{V}_2(\omega) \quad (17)$$

Each input amplitude \hat{V}_1 and \hat{V}_2 can be written in the following form:

$$\hat{V}_1 = V_{cm} + \frac{1}{2}\Delta V, \quad (18)$$

$$\hat{V}_2 = V_{cm} - \frac{1}{2}\Delta V, \quad (19)$$

where $V_{cm} = (\hat{V}_1 + \hat{V}_2)/2$ is the so-called common mode signal and $\Delta V = (\hat{V}_1 - \hat{V}_2)$ is the differential signal.

Using Eqs. (17)–(19), we obtain:

$$\hat{V}_{out} = \hat{A}_d \Delta V + \hat{A}_{cm} V_{cm}, \quad (20)$$

where

$$\hat{A}_d(\omega) = \frac{\hat{A}_1(\omega) - \hat{A}_2(\omega)}{2} \quad (21)$$

and

$$\hat{A}_{cm}(\omega) = \hat{A}_1(\omega) + \hat{A}_2(\omega) \quad (22)$$

In practical operational amplifiers, $|\hat{A}_d(\omega)|$ is much larger than $|\hat{A}_{cm}(\omega)|$ (in the ideal amplifier, $\hat{A}_{cm}(\omega) \equiv 0$). To characterize this very important property, we will use **the common-mode rejection ratio (CMRR)**:

$$\text{CMRR(dB)} = 20 \log \left| \frac{\hat{A}_d}{\hat{A}_{cm}} \right|. \quad (23)$$

Usually, CMRR ~ 80–100 dB.

III. Network measurements of a close loop transfer function

Transfer function $\hat{F}(\omega)$ of an electronic network can be measured by means of a Vector Network Analyser similar to that of the ultrasonic network (see Fig. 3):

$$\hat{F}(\omega) = \hat{A}_f(\omega) = \frac{\hat{V}_{out}(\omega)}{\hat{V}_{in}(\omega)} = S_{21}(\omega) \quad (24)$$

Here, $\hat{V}_{in}(\omega)$ is the voltage amplitude applied from **Port I** of the Analyser to the input of linear network, and $\hat{V}_{out}(\omega)$ is the voltage amplitude (including the phase shift with respect to $\hat{V}_{in}(\omega)$) measured from the

output of linear network at **Port II** of Analyser. The ratio $\frac{\hat{V}_{out}(\omega)}{\hat{V}_{in}(\omega)} = S_{21}(\omega)$ is measured in discrete frequency points (max 1601 points for HP 8753E) within a certain frequency range (max 10 kHz – 6 GHz for HP 8753E). $\hat{V}_{in}(\omega)$ can be considered as a real amplitude of the input reference signal, while $\hat{V}_{out}(\omega)$ will be a complex amplitude due to a phase shift with respect to the input reference signal. Therefore, a Vector Network Analyser in the S_{21} (or S_{12}) configuration measures the complex ratio $\frac{\hat{V}_{out}(\omega)}{\hat{V}_{in}(\omega)}$ (its real and imaginary parts) in discrete frequency points within a certain frequency range. For other frequency points between the sampling ones, the transfer function can be reconstructed by means of a polynomial interpolation.

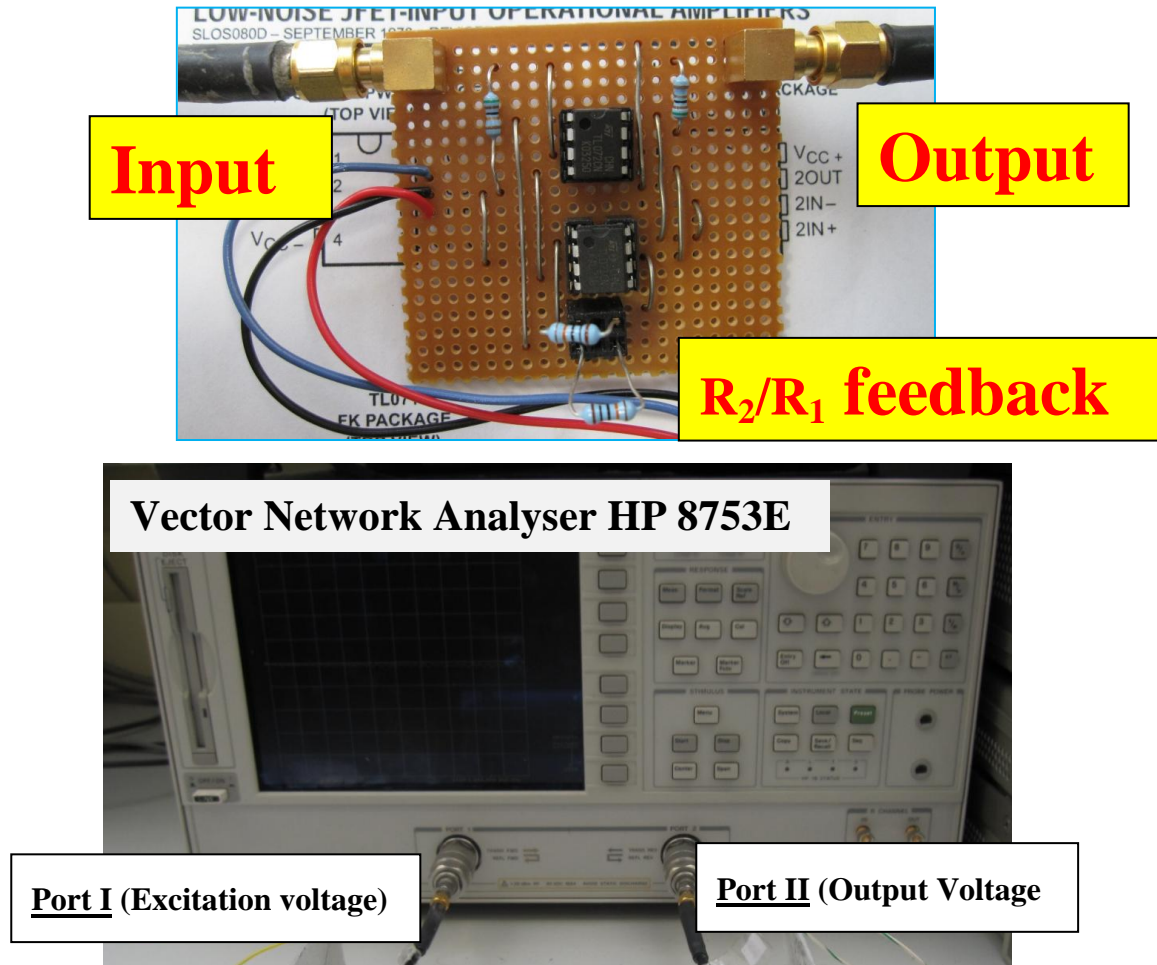


Fig. 3 Network measurements of the transfer function of an electronic network.

To demonstrate the electronic network measurements, we used the circuit shown in Fig. 4: TL071CN-based inverting amplifier (DUT –“device under test”) between two TL072CN-based buffers. We use two buffers at the input and output of DUT to provide the 50 Ω matching with Analyser’s 50 Ω ports. So, our network is a 50 Ω device. Actually, these buffers may also introduce some frequency distortions within the measurement frequency range, i.e. their gain may be not precisely unit. In this case, the total transfer function in the frequency domain will be the product of three transfer functions: DUT, and two

buffers. The $50\ \Omega$ output of our linear network and the Analyser's $50\ \Omega$ input constitute the $1/2$ voltage divider. This is because, at lower frequencies the circuit transfer function will be $-1/2$, not -1 .

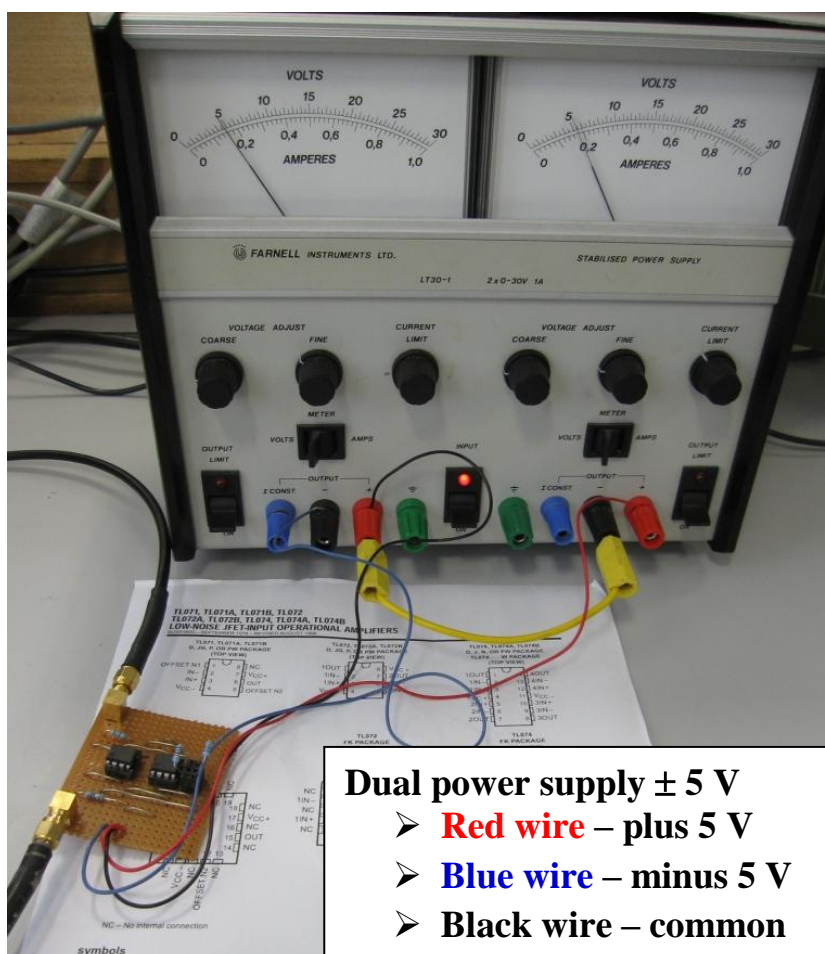
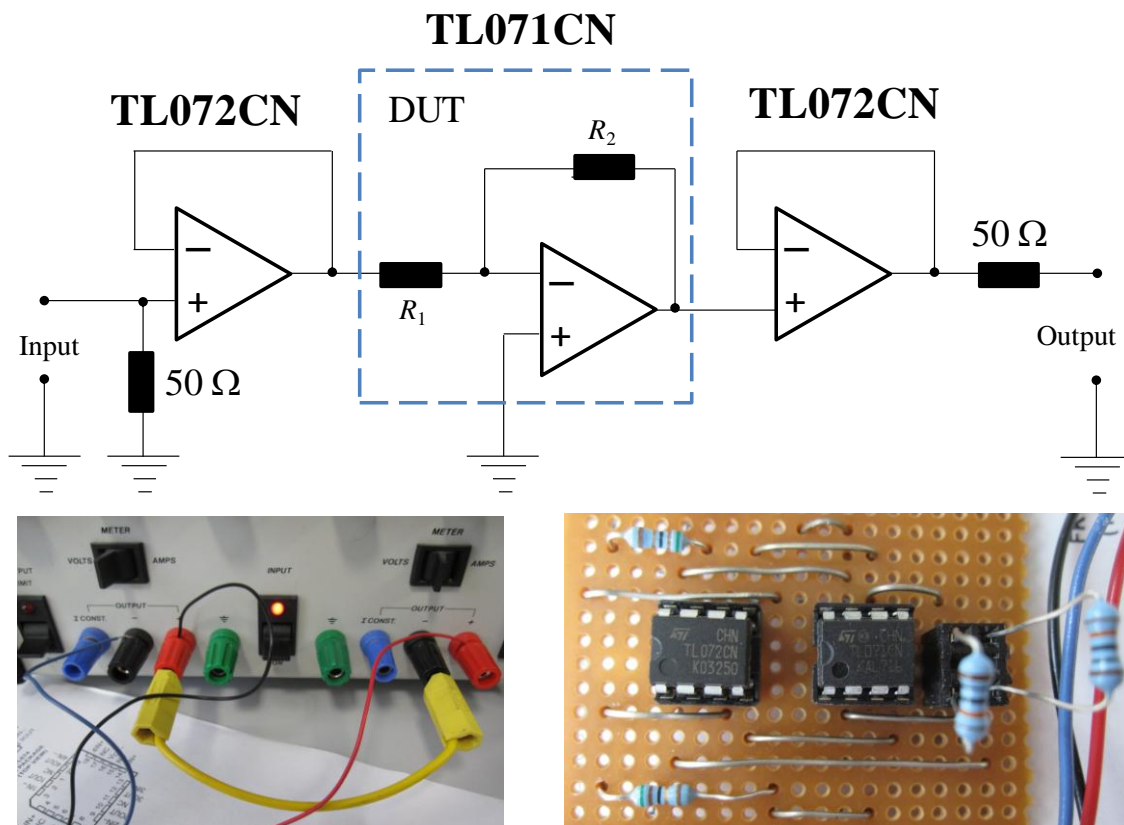
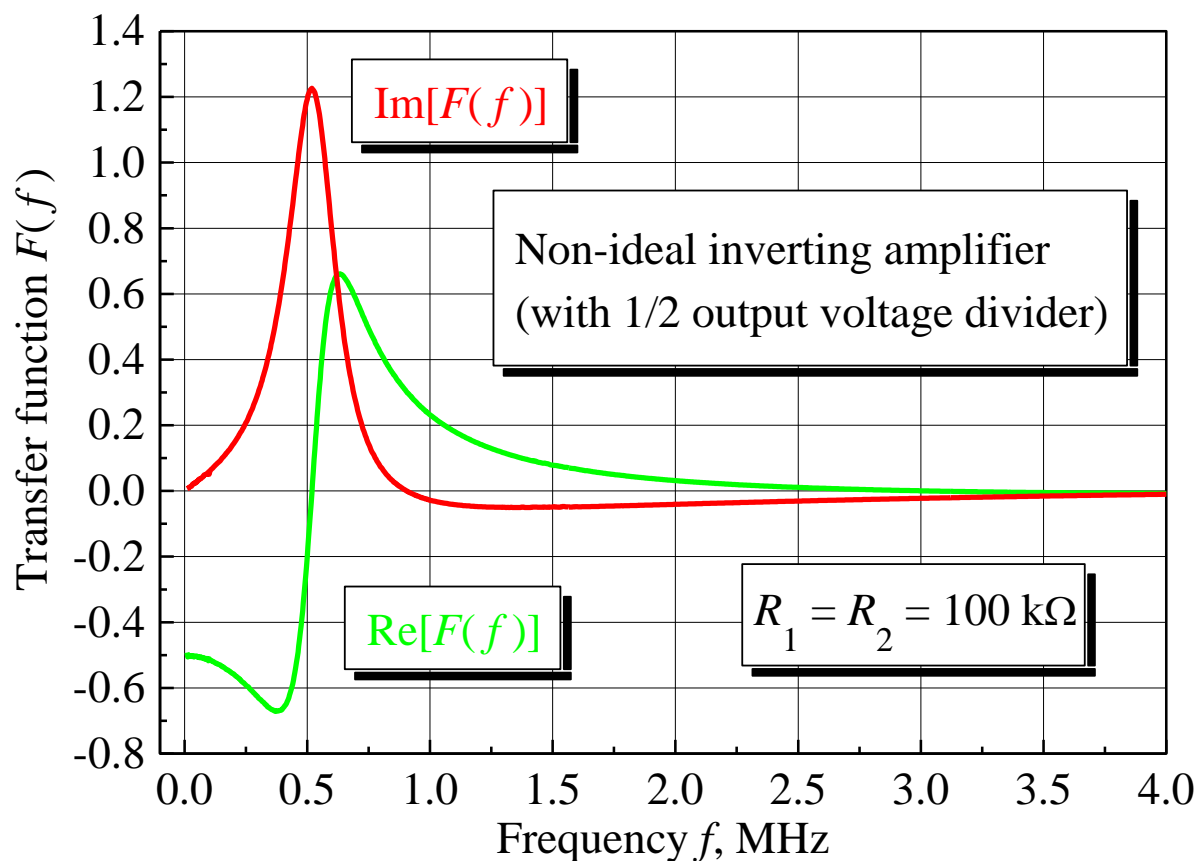
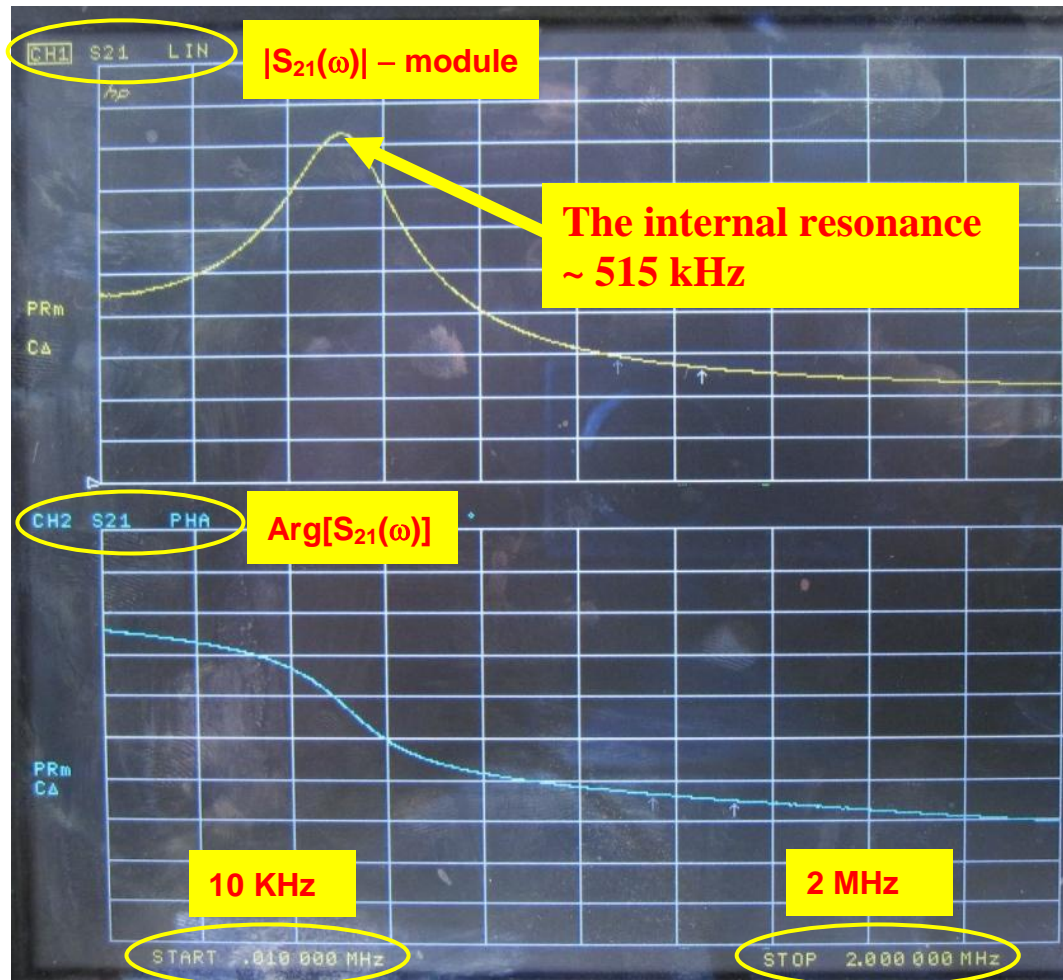


Fig. 4 The electronic network used in the measurements.

The measured magnitude, phase, real and imaginary parts of the transfer function $\hat{F}(\omega) = S_{21}(\omega)$ are shown in Fig. 5 for Gain 1: $R_1 = R_2 = 100 \text{ K}\Omega$.



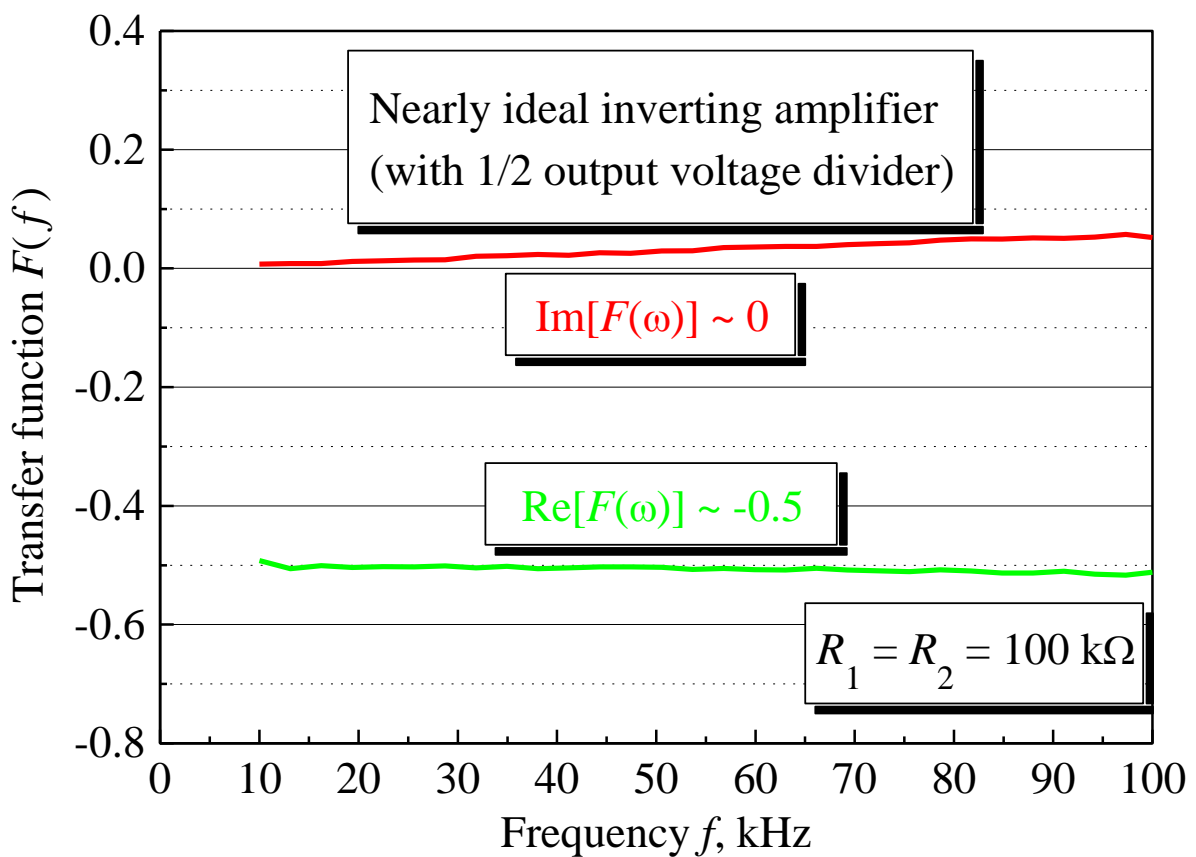
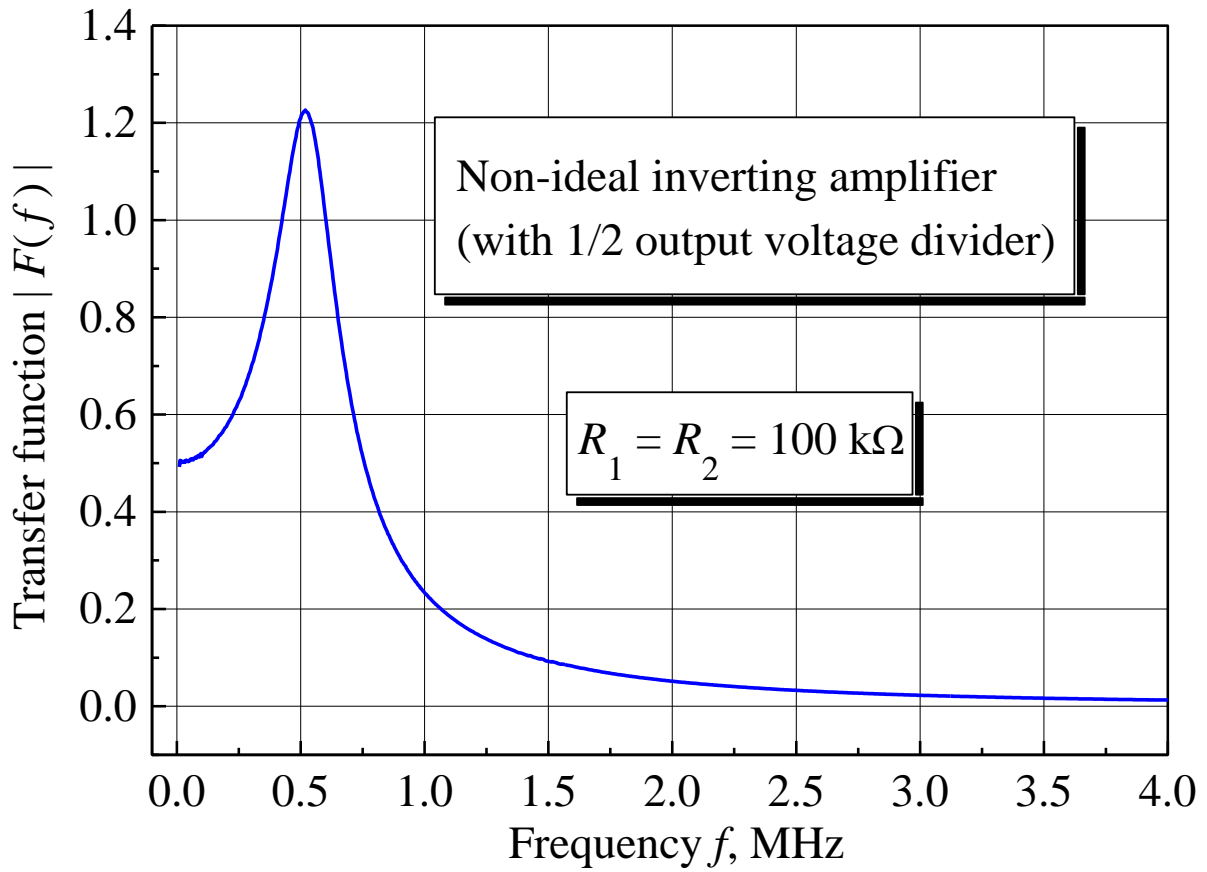


Fig. 5 The magnitude, phase, real, and imaginary parts of the transfer function measured for the electronic network in Fig. 4 (Gain 1).

The main conclusions:

- Only for $f < 100$ kHz, our electronic network ($1 \times \text{TL071CN} + 2 \times \text{TL072CN}$) can be considered as an ideal operational amplifier: the imaginary part of the transfer function is almost zero, and the real part is constant (-0.5 due to the $1/2$ voltage divider).
- Between 250 kHz and 2 MHz, we observe a strong dispersion of the resonance type, with the internal resonance at ~ 515 kHz. Such resonance dispersion is typical for a multi-pole transfer function (two or more poles).
- After 4 MHz, the transfer function is almost zero: no signal propagation.

The pulse responses shown in Fig. 6 reveal strong ringing oscillations. Again, this is a signature of a multi-pole transfer function, since only the transfer function with two or more poles can demonstrate the ringing oscillations (recall Eqs. (13) and (16)).

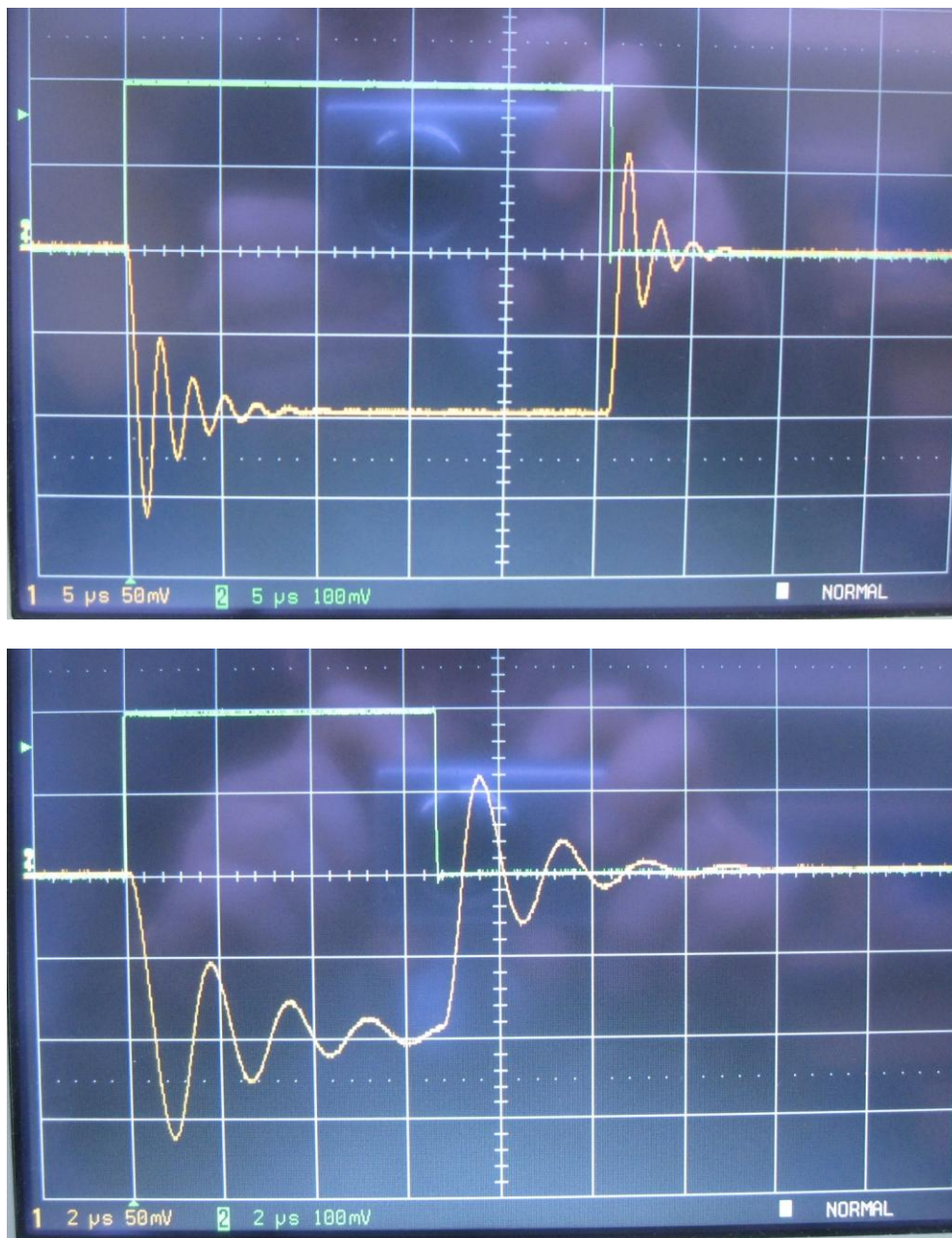


Fig. 6 Pulse response and ringing oscillations measured for the electronic network in Fig. 4 (Gain 1).

Also, the dispersion of transfer function introduces a strong frequency distortion (**brown curve**), as shown in Fig. 7 for the triangle excitation (**green curve**).

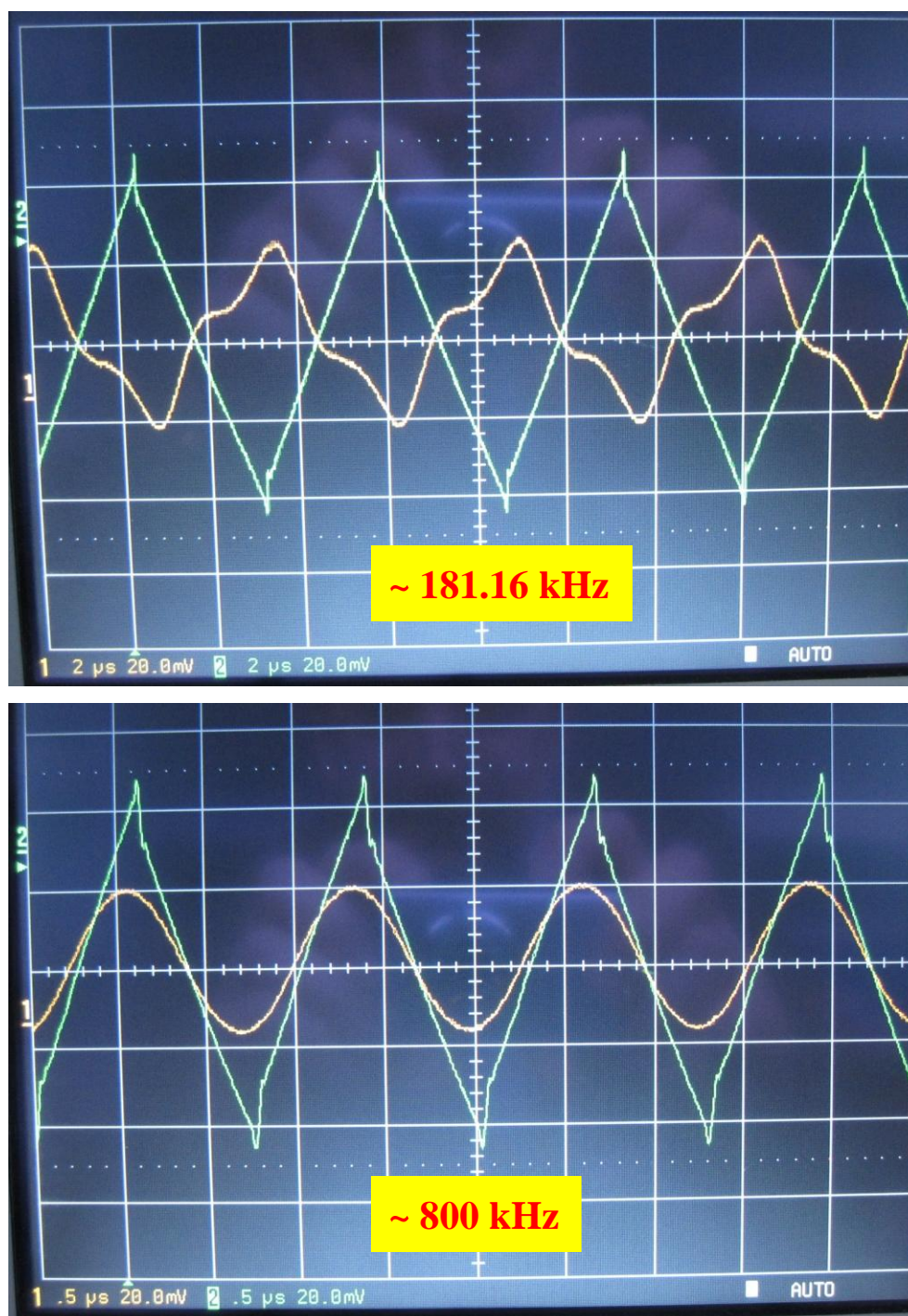


Fig. 7 Frequency distortion measured for the triangle excitation for the electronic network in Fig. 4 (Gain 1).

For a non-inverting amplifier, we can use another measurement scheme shown in Fig. 6.

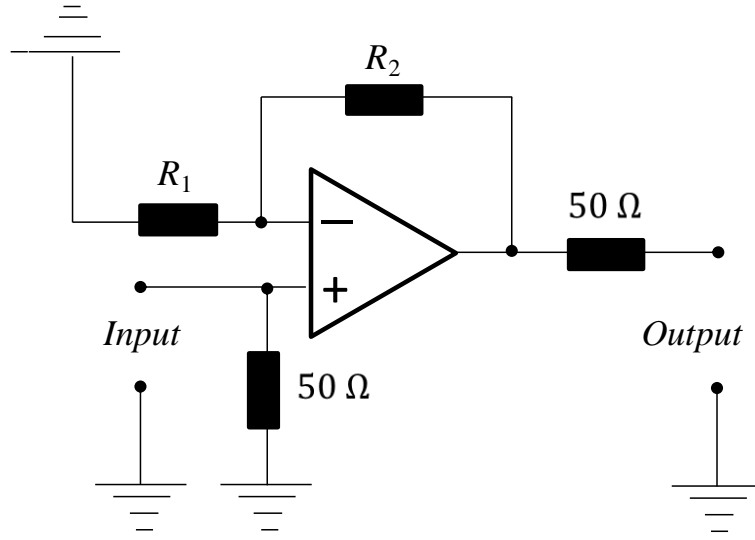


Fig. 8 Network measurements of the transfer function of a non-inverting operational amplifier.

IV. Calculation of the time domain transfer function and the time domain responses

For an electronic network, the equation $F(t > 0) = 2 \int_0^{+\infty} (\text{Re}[\hat{F}(f)] \cos(2\pi f t) - \text{Im}[\hat{F}(f)] \sin(2\pi f t)) df$

has to be modified since our Network Analyser cannot conduct the measurements below 10 kHz. However, from 0 to $f_1 = 10$ kHz the transfer function of our network is almost constant and its imaginary part is zero. Therefore, the integration can be divided into two parts:

$$\begin{aligned}
 F(t > 0) &= 2 \int_0^{+\infty} (\text{Re}[\hat{F}(f)] \cos(2\pi f t) - \text{Im}[\hat{F}(f)] \sin(2\pi f t)) df \approx \\
 &\approx 2 \int_0^{f_1} (\text{Re}[\hat{F}(f)] \cos(2\pi f t) - \text{Im}[\hat{F}(f)] \sin(2\pi f t)) df + 2 \int_{f_1}^{f_N} (\text{Re}[\hat{F}(f)] \cos(2\pi f t) - \text{Im}[\hat{F}(f)] \sin(2\pi f t)) df \approx \\
 &\approx 2 \text{Re}[\hat{F}(f_1)] \times \int_0^{f_1} \cos(2\pi f t) df + 2 \int_{f_1}^{f_N} (\text{Re}[\hat{F}(f)] \cos(2\pi f t) - \text{Im}[\hat{F}(f)] \sin(2\pi f t)) df = \\
 &= 2 \text{Re}[\hat{F}(f_1)] \times \frac{\sin(2\pi f_1 t)}{2\pi t} + 2 \int_{f_1}^{f_N} (\text{Re}[\hat{F}(f)] \cos(2\pi f t) - \text{Im}[\hat{F}(f)] \sin(2\pi f t)) df
 \end{aligned}$$

$$F(t > 0) \approx 2 \text{Re}[\hat{F}(f_1)] \times \frac{\sin(2\pi f_1 t)}{2\pi t} + 2 \int_{f_1}^{f_N} (\text{Re}[\hat{F}(f)] \cos(2\pi f t) - \text{Im}[\hat{F}(f)] \sin(2\pi f t)) df \quad (25)$$

$$\left. \frac{\sin(2\pi f_1 t)}{2\pi t} \right|_{t \rightarrow 0} = f_1$$

where $f_N \sim 4-5$ MHz (for this particular network) and $N=1601$ for HP 8753E. Now, Eq. (25) can be used for the numerical calculations (see **Appendix 1**).

We have calculated $F(t > 0)$ for the electronic network in Fig. 4 with Gain 1: $R_1 = R_2 = 100 \text{ K}\Omega$ (see Fig. 9).

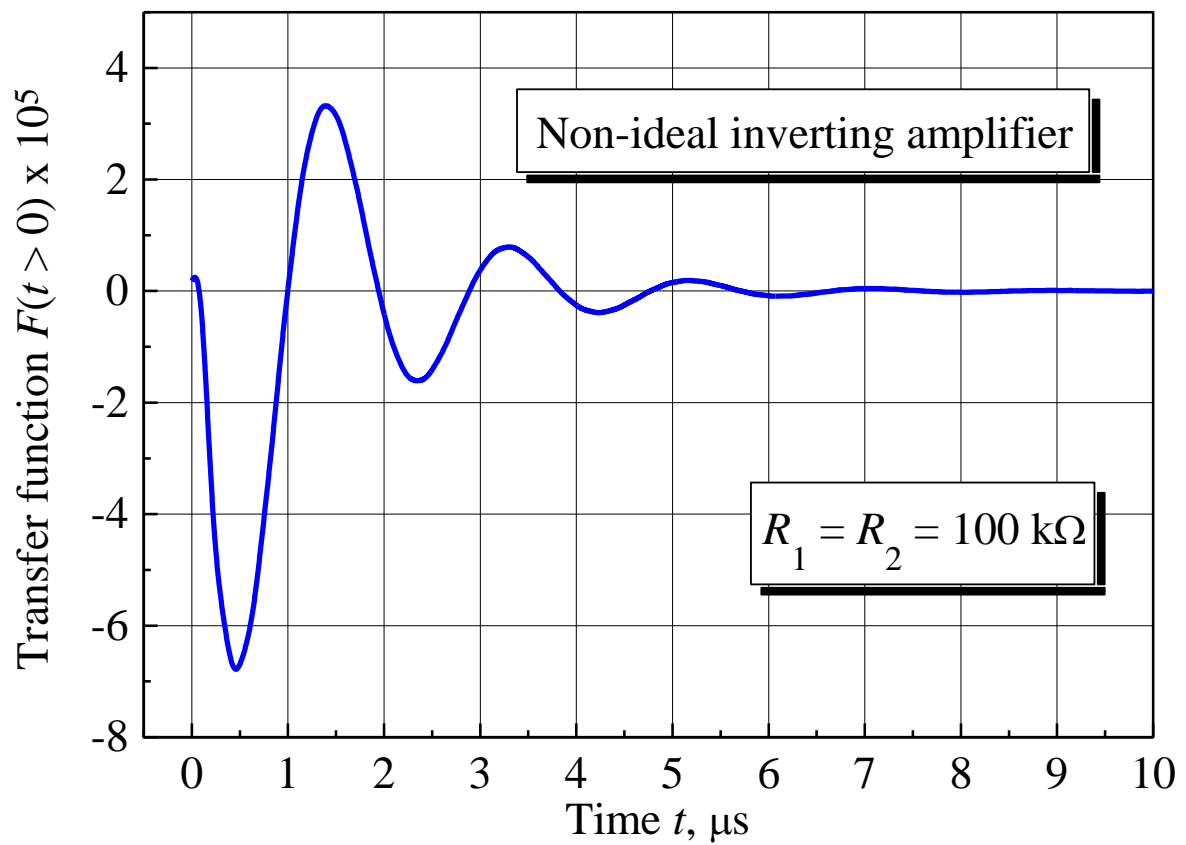


Fig. 9 The time domain transfer function calculated for the electronic network in Fig. 4 (Gain 1).

Compare this $F(t > 0)$ with the measured short pulse response, shown in Fig. 10.

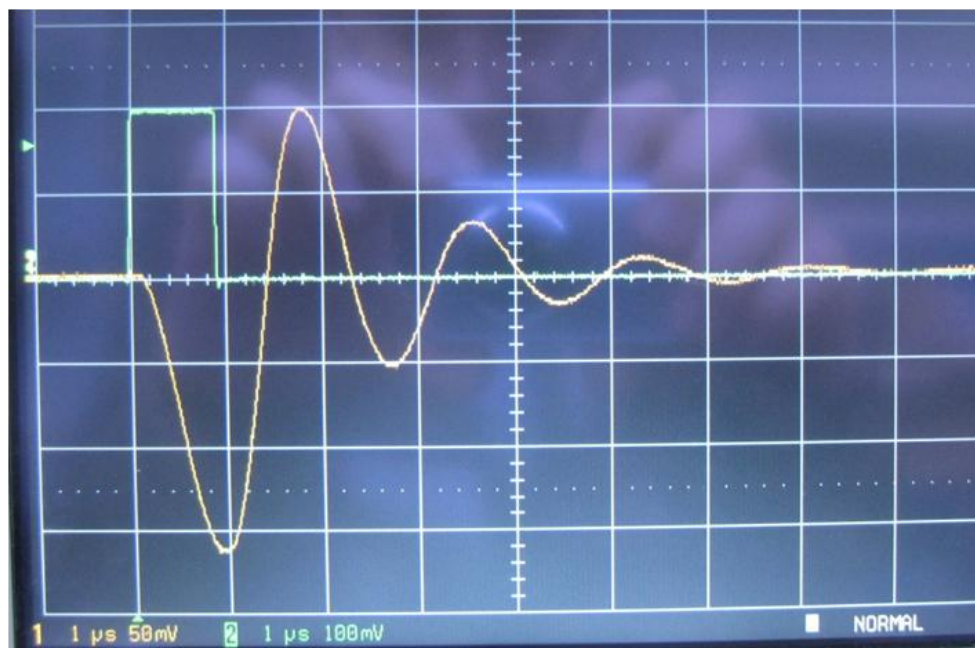


Fig. 10 A short pulse response measured for the electronic network in Fig. 4 (Gain 1).

A very short single pulse applied at $t=0$ can be approximated by Dirac's delta function: $V_{in}(t) \sim \delta(t)$.

Putting this approximation into the convolution, we obtain: $V_{out}(t) \approx \int_{-\infty}^t F(t-s)\delta(s)ds = F(t)$. **Therefore, a short pulse excitation can be used for the experimental observation of $F(t)$.**

The measured $\hat{F}(f)$ can be used for calculations of a pulse or periodical response. For the pulse response, we can use the equation $V_{out}(t) = 2 \int_0^{+\infty} \text{Re}[\hat{F}(f)\hat{V}_{in}(f)\exp(i2\pi f t)]df$, but again it has to be modified:

$$\begin{aligned} V_{out}(t) &= 2 \int_0^{+\infty} \text{Re}[\hat{F}(f)\hat{V}_{in}(f)\exp(i2\pi f t)]df = 2 \int_0^{f_1} \text{Re}[\hat{F}(f)\hat{V}_{in}(f)\exp(i2\pi f t)]df + \\ &+ 2 \int_{f_1}^{+\infty} \text{Re}[\hat{F}(f)\hat{V}_{in}(f)\exp(i2\pi f t)]df \approx 2 \text{Re}[\hat{F}(f_1)] \times \int_0^{f_1} \text{Re}[\hat{V}_{in}(f)\exp(i2\pi f t)]df + \\ &+ 2 \int_{f_1}^{f_N} \text{Re}[\hat{F}(f)\hat{V}_{in}(f)\exp(i2\pi f t)]df \end{aligned}$$

$$V_{out}(t) \approx 2 \text{Re}[\hat{F}(f_1)] \times \int_0^{f_1} \text{Re}[\hat{V}_{in}(f)\exp(i2\pi f t)]df + 2 \int_{f_1}^{f_N} \text{Re}[\hat{F}(f)\hat{V}_{in}(f)\exp(i2\pi f t)]df \quad (26)$$

Both the integrals in Eq. (26) can be calculated numerically using the piecewise linear interpolation of $\text{Re}[\hat{V}_{in}(f)\exp(i2\pi f t)]$ and $\text{Re}[\hat{F}(f)\hat{V}_{in}(f)\exp(i2\pi f t)]$ (see **Appendix 2**). Here:

$$\begin{cases} \hat{V}_{in}(f) = \frac{\sin(2\pi f T)}{2\pi f} + i \frac{(\cos(2\pi f T) - 1)}{2\pi f} \\ \hat{V}_{in}(0) = T \end{cases}$$

is the Fourier image of the unit square positive pulse and T is its width.

The Fourier series for the positive pulses also can be used to calculate a single pulse response, if $\tau_p \gg \tau_w$ (τ_w is the pulse width, τ_p is the pause between pulses, and $T = \tau_w + \tau_p$ is the period):

$$\left\{ \begin{aligned} V_{in}(t) &= \frac{a_0}{2} + \sum_{k=1}^{\infty} \left[a_k \cos\left(\frac{2\pi k}{\tau_w + \tau_p} t\right) + b_k \sin\left(\frac{2\pi k}{\tau_w + \tau_p} t\right) \right] \\ \frac{a_0}{2} &= \frac{A \tau_w}{\tau_w + \tau_p} \\ a_k &= \frac{A}{k\pi} \sin\left(\frac{2\pi k \tau_w}{\tau_w + \tau_p}\right) \\ b_k &= \frac{A}{k\pi} \left(1 - \cos\left(\frac{2\pi k \tau_w}{\tau_w + \tau_p}\right)\right) \end{aligned} \right. \quad (27)$$

In this case ($\tau_p \gg \tau_w$), we avoid a strong interference between the pulses, and hence each of them can be considered as an individual pulse:

$$\left\{ \begin{aligned} V_{out}(t) &= \text{Re}[\hat{F}(0)] \frac{a_0}{2} + \\ &+ \sum_{m=1}^{\infty} \left[\left(a_m \text{Re}[\hat{F}(f_m)] + b_m \text{Im}[\hat{F}(f_m)] \right) \cos(\omega_m t) + \left(b_m \text{Re}[\hat{F}(f_m)] - a_m \text{Im}[\hat{F}(f_m)] \right) \sin(\omega_m t) \right] \\ T &= \tau_w + \tau_p; \quad f = \frac{1}{T}; \quad f_m = f \times m = \frac{m}{T}; \quad \omega_m = 2\pi f_m \end{aligned} \right. \quad (28)$$

In Eq. (28), for any $f < f_1 = 10$ KHz we will assume that $\text{Re}[\hat{F}(f)] \approx \text{Re}[\hat{F}(f_1)]$ and $\text{Im}[\hat{F}(f)] \approx 0$. Also, $\hat{F}(f)$ must be interpolated between its sampling frequency points f_k (**1601 points for HP 8753E Network Analyser**) to calculate $\text{Re}[\hat{F}(f)]$ and $\text{Im}[\hat{F}(f)]$ in any frequency point f . Note that the harmonic frequencies f_m in the Fourier series will not coincide with the sampling points f_k . The linear approximation $\hat{F}_k^{k+1}(f)$ of $\hat{F}(f)$ for each elementary frequency interval $[f_k, f_{k+1}]$ is:

$$\left\{ \begin{aligned} \hat{F}_k^{k+1}(f) &= \frac{\hat{F}(f_k) \times f_{k+1} - \hat{F}(f_{k+1}) \times f_k}{f_{k+1} - f_k} + \frac{\hat{F}(f_{k+1}) - \hat{F}(f_k)}{f_{k+1} - f_k} \times f \\ k &= 1, N-1 \end{aligned} \right.$$

where N is the total number of frequency points, $\hat{F}_k^{k+1}(f_k) = \hat{F}(f_k)$ and $\hat{F}_k^{k+1}(f_{k+1}) = \hat{F}(f_{k+1})$. The continuous approximation $\tilde{F}(f)$ of $\hat{F}(f)$ is represented as the weighted sum of $\hat{F}_k^{k+1}(f)$:

$$\tilde{F}(f) = \sum_{k=1}^{N-1} \theta_k^{k+1}(f) \hat{F}_k^{k+1}(f)$$

where

$$\theta_k^{k+1}(f) = \begin{cases} 1, & f \in [f_k, f_{k+1}] \\ 0, & f \notin [f_k, f_{k+1}] \end{cases} \quad \text{-- is the frequency interval numerator.}$$

Using Eqs. (27),(28), we have calculated the pulse response for the electronic network in Fig. 4 with Gain 1: $R_1 = R_2 = 100$ K Ω (see Fig. 11). An excellent agreement with the measured signal has been

achieved: compare with Fig. 6. These calculations can be used to determine the slew rate of the electronic network, as it is explained in Fig. 12. **To observe ringing oscillations, the slew rate of the excitation pulse must be higher than the slew rate of the electronic network, i.e. “a sharp pulse”.** Increasing the gain ($R_1 < R_2$), we will suppress ringing oscillations and decrease the slew rate of the electronic network (recall our practical work on operational amplifiers). For example, for Gain 10 ($R_1 = 10 \text{ K}\Omega$ and $R_2 = 100 \text{ K}\Omega$) our network will not demonstrate any ringing oscillations and the output pulses will be smooth.

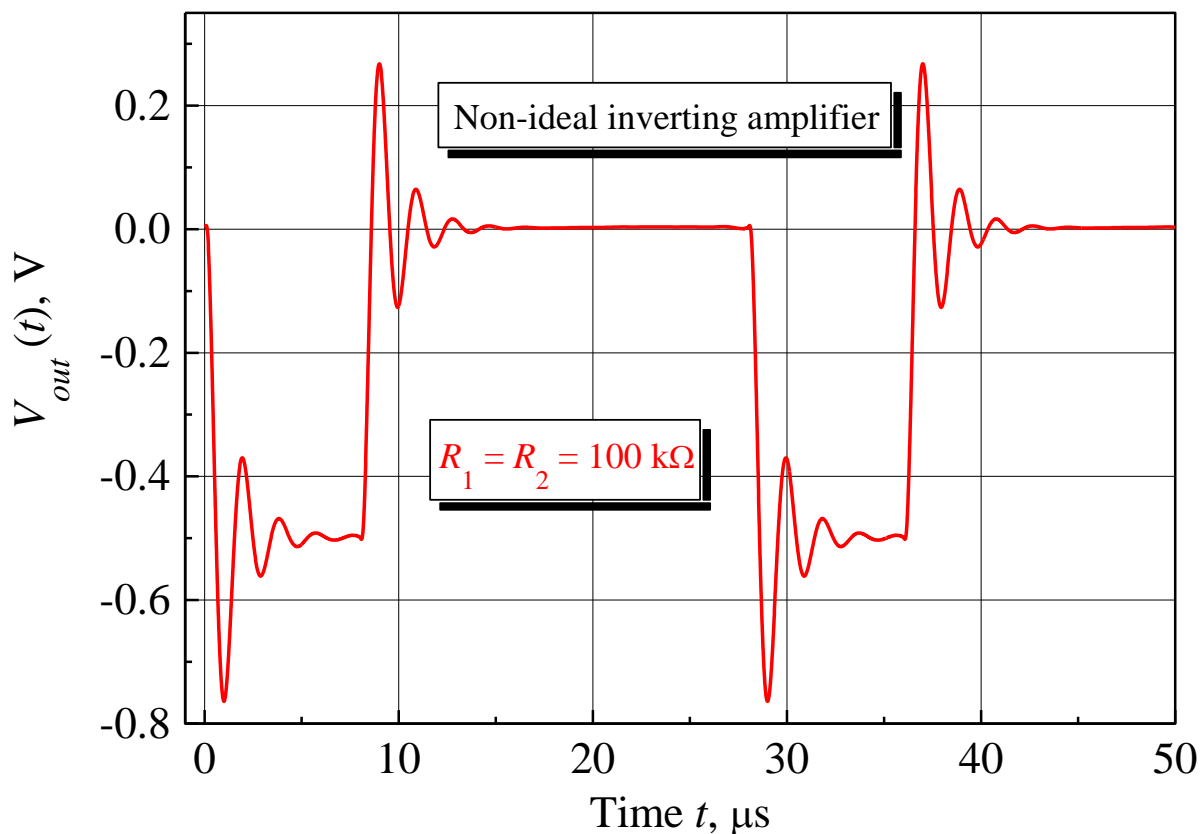


Fig. 11 A pulse response calculated for the electronic network in Fig. 4 (Gain 1) using Eqs. (27),(28).

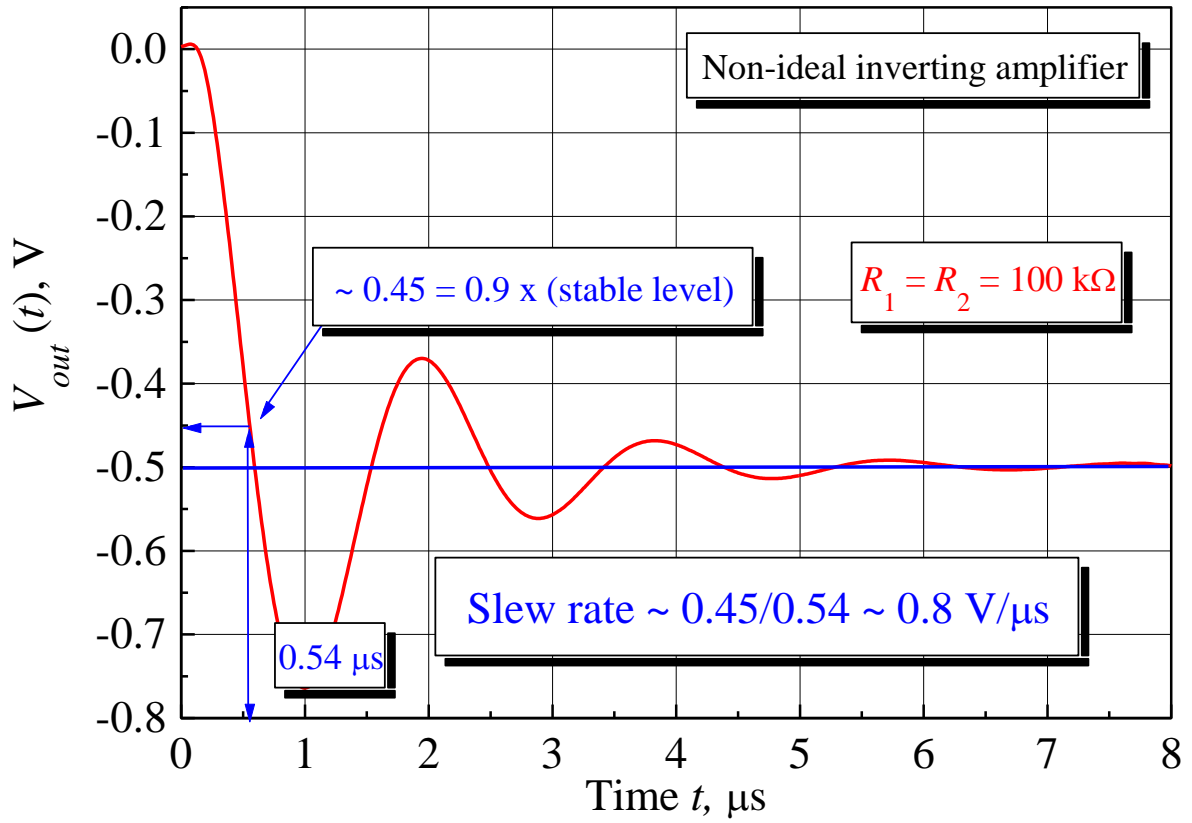
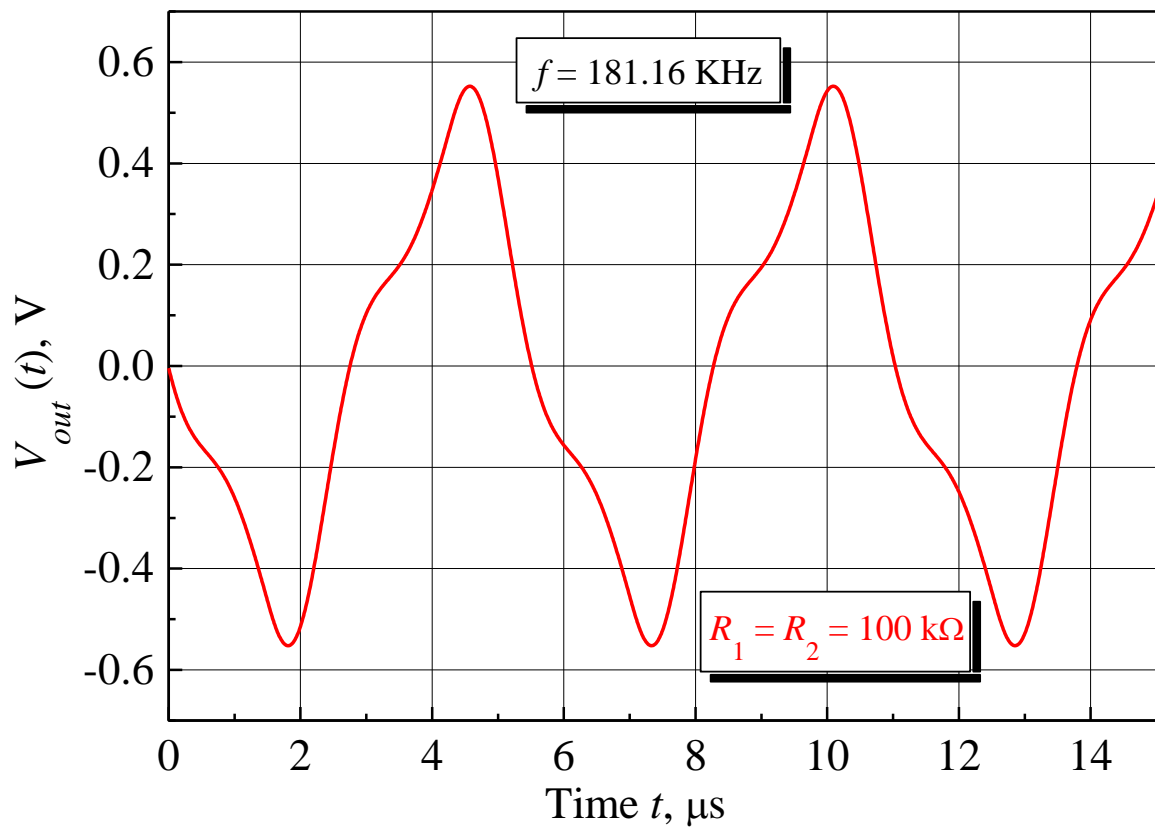


Fig. 12 Calculation of the slew rate for the electronic network in Fig. 4 (Gain 1).

Using the same equations (27),(28), we have calculated the periodical response for the triangle excitation for the electronic network in Fig. 4 with Gain 1: $R_1 = R_2 = 100 \text{ K}\Omega$ (see Fig. 13). A strong frequency distortion is observed for the excitation frequencies above 20 KHz.



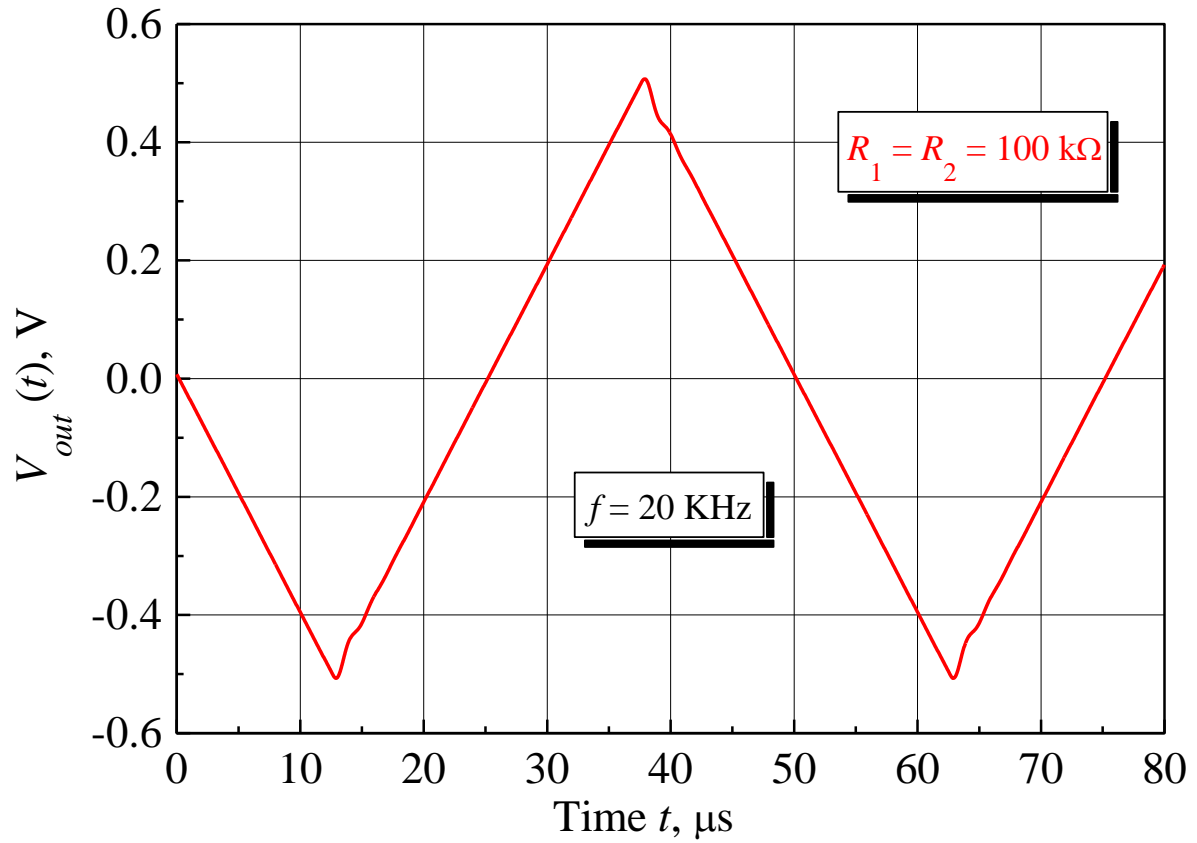


Fig. 13 The periodical response calculated for the triangle excitation for the electronic network in Fig. 4 (Gain 1) using Eqs. (27),(28).

Appendix 1: Fortran program for the calculation of the time domain transfer function

```

c
c | The linear interpolation of F(f) - transfer function in the frequency domain
c
c Calculation of the time domain transfer function F(t) from the experimental F(f)
c
USE MSISLMD
INTEGER N,Nf,Nt
DOUBLE PRECISION t0

c N is the number of frequency sampling points for F(f)
PARAMETER (N=1601)
c Nf=N-1 is the number of frequency intervals
PARAMETER (Nf=1600)
c Nt is the number of time intervals for F(t)
PARAMETER (Nt=5000)
c t0 is the maximum time: t=[0,t0]
PARAMETER (t0=10.0E-6)

DOUBLE PRECISION f(N),ReF(N),ImF(N),pi
DOUBLE PRECISION A(Nf),B(Nf),C(Nf),D(Nf),at,t,Ft
INTEGER m,q

pi=3.1415926535897932384626433832795

OPEN(10,FILE='OpAmp.dat')
DO m=1,N
    READ(10,*) f(m),ReF(m),ImF(m)
END DO
CLOSE(10)

DO m=1,Nf
    A(m)=(ReF(m)*f(m+1)-ReF(m+1)*f(m))/(f(m+1)-f(m))
    B(m)=(ReF(m+1)-ReF(m))/(f(m+1)-f(m))
    C(m)=(ImF(m)*f(m+1)-ImF(m+1)*f(m))/(f(m+1)-f(m))
    D(m)=(ImF(m+1)-ImF(m))/(f(m+1)-f(m))
END DO

```

```

OPEN(20,FILE='Time Domain.dat')

t=0.0
Ft=2*ReF(1)*f(1)
DO q=1,Nf
    Ft=Ft+(ReF(q)+ReF(q+1))*(f(q+1)-f(q))
END DO

WRITE(20,*) t,Ft

DO m=1,Nt

    WRITE(*,*) m
    t=(t0/Nt)*m
    at=2.0*pi*t

    Ft=0.0
    DO q=1,Nf
        Ft=Ft+A(q)*(DSIN(at*f(q+1))-DSIN(at*f(q)))/at
        Ft=Ft+B(q)*(f(q+1)*DSIN(at*f(q+1))-f(q)*DSIN(at*f(q)))/at
        Ft=Ft+B(q)*(DCOS(at*f(q+1))-DCOS(at*f(q)))/(at**2)
        Ft=Ft-C(q)*(DCOS(at*f(q))-DCOS(at*f(q+1)))/at
        Ft=Ft-D(q)*(f(q)*DCOS(at*f(q))-f(q+1)*DCOS(at*f(q+1)))/at
        Ft=Ft-D(q)*(DSIN(at*f(q+1))-DSIN(at*f(q)))/(at**2)
    END DO

    Ft=2.0*Ft+2.0*ReF(1)*DSIN(2.0*pi*f(1)*t)/(2.0*pi*t)

    WRITE(20,*) t,Ft

END DO

CLOSE(20)

STOP
END

```

Appendix 2: Fortran program for the calculation of a single pulse response

```

c
c      A single pulse response Vout(t)
c
c      Calculation of Vout(t) from the experimental F(f) and the pulse Fourier image Vin(f)
c
c
c      USE MSIMSLMD
c      INTEGER N,N1,Nt
c      DOUBLE PRECISION t0,pw
c
c      N is the number of frequency sampling points for F(f)
c      ■ PARAMETER (N=1601)
c      N1 is the number of frequency points for the low frequency integration, i.e.
c      below f(1) in the spectrum of F(f)
c      ■ PARAMETER (N1=100)
c      Nf=N-1 is the number of frequency intervals
c      ■ PARAMETER (Nt=5000)
c      t0 is the maximum time: t=[0,t0] (seconds)
c      ■ PARAMETER (t0=28.0E-6)
c      pw is the pulse width (seconds)
c      ■ PARAMETER (pw=8.0E-6)
c
c      DOUBLE PRECISION f(N),f1(N1),ReF(N),ImF(N),H(N),H1(N1),pi,t,Vout
c      DOUBLE PRECISION par
c      DOUBLE COMPLEX cunit,unit,Vin
c      INTEGER m,q
c      COMMON /par/ par
c      EXTERNAL Vin
c
c      pi=3.1415926535897932384626433832795
c      Real unit 1.0
c      ■ unit=(1.0,0.0)
c      Complex unit i=SQRT(-1)
c      cunit=(0.0,1.0)
c      par=pw
c
c      OPEN(10,FILE='OpAmp_R_G1.dat')
c      DO m=1,N
c          READ(10,*) f(m),ReF(m),ImF(m)
c      END DO
c      CLOSE(10)

```

```

DO m=1,N1
  fl(m)=f(1)*(m-1)/(N1-1)
END DO

OPEN(20,FILE='Pulse response.dat')

DO m=0,Nt
  WRITE(*,*) m
  t=(t0/Nt)*m

  DO q=1,N
    H(q)=DBLE((unit*ReF(q)+cunit*ImF(q))*Vin(f(q))*
      CDEXP(cunit*2.0*pi*f(q)*t))
  END DO

  DO q=1,N1
    Hl(q)=ReF(1)*DBLE(Vin(fl(q))*CDEXP(cunit*2.0*pi*fl(q)*t))
  END DO

  Vout=0.0
  DO q=1,N-1
    Vout=Vout+(H(q)+H(q+1))*(f(q+1)-f(q))
  END DO

  DO q=1,N1-1
    Vout=Vout+(Hl(q)+Hl(q+1))*(fl(q+1)-fl(q))
  END DO

  WRITE(20,*) t,Vout
END DO

CLOSE(20)

STOP
END

```

```

A single pulse Fourier image; Eq.(A1) in Lecture 3
FUNCTION Vin(f)
DOUBLE COMPLEX Vin,unit,cunit
DOUBLE PRECISION f,pi,par,pw
COMMON /par/ par

pi=3.1415926535897932384626433832795
unit=(1.0,0.0)
cunit=(0.0,1.0)
pw is the pulse width (seconds)
pw=par

IF(f.EQ.0.0) THEN
  Vin=par*unit
ELSE
  Vin=DSIN(2.0*pi*f*pw)*unit/(2.0*pi*f)
  Vin=Vin+cunit*(DCOS(2.0*pi*f*pw)-1.0)/(2.0*pi*f)
END IF

RETURN
END

```